MNDO/H and AM1 Studies of Nitro Enamines with Intramolecular Hydrogen Bonds

Enrique Sánchez Marcos,[a,*] José Joaquín Maraver,[a] José Luis Chiara,[b] and Antonio Gómez-Sánchez[b]
[a] *Departamento de Química Física, Universidad de Sevilla, Apartado de Correos No. 553, 41071-Sevilla, Spain*
[b] *Instituto de la Grasa y sus Derivados, C.S.I.C., and Departamento de Química Orgánica, Universidad de Sevilla, Apartado de Correos No. 553, 41071-Sevilla, Spain*

A set of nitro enamines with intramolecular hydrogen bonding have been studied by the MNDO/H and the AM1 method. Geometries, isomer populations, and rotational barriers around the carbon–carbon double bond predicted by the calculations are compared with experimental results. Solvent effects on isomeric equilibria are considered. It is shown that semiempirical calculations supply a reasonable description of the static and dynamic properties of these systems, although accurate predictions are possible only by including solvent effects.

The study of nitro enamines has recently been stimulated by the potential use of these compounds in organic synthesis.[1–4] These alkenes are typical push–pull ethylenes,[5] since they have the strongly electron-donating amino group attached to one side of the double bond and the strongly electron-withdrawing nitro group on the other side. This implies that *cis–trans* isomerization is generally characterized by low energy barriers, and that the stereochemistry of their reactivity may be controlled by the relative population of isomers. Nitro enamines containing a primary or secondary amino group lead to more complicated systems where intramolecular hydrogen bonding between the amino and nitro groups may be formed, the *cis* isomer being favoured in these cases. An additional proton-accepting group on the carbon bearing the nitro group leads to molecules in which both configurational isomers have hydrogen-bonding interactions, and the isomer-ratio prediction is more difficult. In these systems, spectroscopic information is partly clouded owing to the difficulty of assigning bands to the different isomers involved in the equilibrium. Furthermore, as it has been reported for other push–pull ethylenes,[5–9] the isomer ratio and the interconversion energy barriers are strongly dependent on the solvent.[10–13]

Theoretical studies allow a separation of the contribution of the different isomers to the equilibrium by an individualized analysis of each possible species present. The comparison of experimental evidence and theoretical predictions may offer a deeper insight into the problem. Thus, in the study of other push–pull ethylenes,[5,13–16] calculations have proved to be very useful in analysing the relative importance of the different factors determining the static and dynamic properties of the isomeric equilibria.

In relation to nitro enamines, Gate *et al.*[13] carrying out STO-3G *ab initio* calculations on *N*-methyl-2-nitroethenamine have found that the intramolecularly bonded *Z*-isomer is the most stable structure, and that the isomer ratio correlates well with their n.m.r. experiments. From calculations at the CNDO/2 level of the interconversion barrier around the double bond of methyl 3-methylamino-2-nitroacrylate, Borisov *et al.*[14] concluded that the *Z*-isomer is energetically (8 kcal mol^{-1}) more favoured than the *E*-isomer, and that the calculated barrier of 54 kcal mol^{-1} is three times that at the experimental value (15 kcal mol^{-1}), ascribing the differences to solvent effects.

In this paper a set of structurally related nitro enamines (**1**)—(**7**), with intramolecular hydrogen bonding, have been studied theoretically. All these compounds were recently characterized and thoroughly studied using several spectroscopic techniques (i.r., Raman, and n.m.r.). Compound (**1**) exclusively adopts the *Z* configuration when dissolved in chloroform, but the *Z*:*E* ratio decreases when the solvent polarity increases, reducing to 3:1 and 2:1 in methanol and dimethyl sulphoxide, respectively.[17,18] Compound (**2**), as well as its *N*-methyl derivative (**6**), gives a 1:1 ratio of configurational isomers in chloroform, but in more polar solvents, such as dimethyl sulphoxide, the equilibrium is shifted towards the *Z*-forms, especially favouring the *ZE* population.[10,19] Compounds (**3**) and (**7**) adopt only one conformation in each of the configurational *Z*- and *E*-form; the former, having the ester group not coplanar with the rest of the conjugated system, predominates in non-polar solvent.[18] The *N*-alkyl derivatives of (**4**) and (**5**) exist preferentially in the *EZ*-form in chloroform solution.[18,20]

The *Z*,*E* isomerization of enamines with primary or secondary amino groups may proceed either through a thermal mechanism or by a proton-exchange reaction involving the anion.[10] The calculations performed correspond to a thermal isomerization, therefore the results should be compared with the experimental information concerning this mechanism. In acetonitrile, the barrier found[11,12] for compound (**2**) is greater than 21 kcal mol^{-1}, and for compound (**6**) it is 18 kcal mol^{-1}; for the *N*-methyl derivative of (**4**) the energy barrier in *o*-dichlorobenzene is 19 kcal mol^{-1}.[18] Qualitative estimations[18] for compounds (**3**) and (**7**) indicate barriers close to 10—11 kcal mol^{-1} and 8—9 kcal mol^{-1}, respectively, in chloroform.

In the present study attention has been focussed on the equilibria between the different configurational and conformational isomers (see Scheme 1), as well as on the energy barrier of the interconversion between these isomers. Likewise, given the strong solvent effects on the equilibria, the solvation energy for compounds (**1**), (**2**), and (**3**), as a function of solvent polarity, has been calculated.

Method of Calculation.—A semiempirical method is appropriate for this study, especially since extensive geometry optimizations are required for a meaningful assessment of isomerization energies. Although MNDO[21] appears reliable in estimating the heats of formation and rotation barriers of ethylene and related compounds, it fails to predict acceptable hydrogen bonds. For this reason, the total energy of each

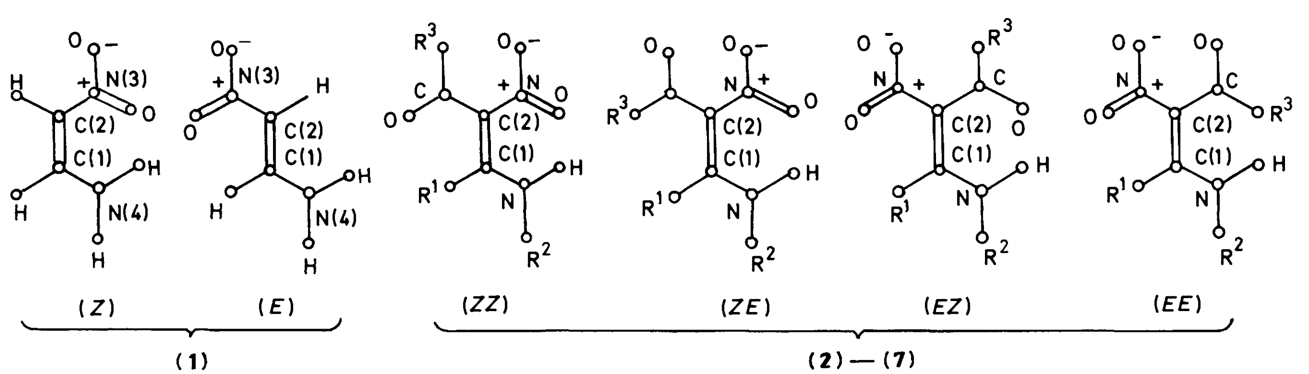

Scheme 1.*

	R^1	R^2	R^3
(2)	H	H	OMe
(3)	H	H	OMe
(4)	H	H	Me
(5)	Me	H	Me
(6)	H	Me	OMe
(7)	Me	Me	OMe

molecule considered was computed by MNDO/H,[22] a modified version of MNDO for the treatment of hydrogen-bonded species, and by the recently developed AM1.[23] For the simplest compound, *i.e.* (**1**), STO-3G and 3-21G calculations were also carried out in order to make a comparison between the semiempirical and *ab initio* results, and to ascertain which of the methods are more suitable for describing the structural and energetic aspects of the different isomers involved in the equilibria.

The equipotential-cavity model, developed by Rivail *et al.*,[24] was used to study the solvent effects on the conformational equilibria. The molecule is included in a cavity surrounded by a polarizable continuum, which models the solvent, with a static dielectric permittivity ε. The solvation energy is defined as the variation of the free energy of the sample when the molecule is placed in the cavity. This quantity is half the electrostatic interaction energy of the molecule with the continuum polarized by the charge distribution of the molecule itself, and can be written:

$$F = \frac{1}{2}\int_{\text{cavity}} v(\vec{r})\rho_0(r)\mathrm{d}\tau$$

where ρ_0 is the charge density of the molecule and $v(\vec{r})$ is the electrostatic potential created inside the cavity by the continuum. Tomasi *et al.*[25] have shown that the potential $v(\vec{r})$ can be conveniently computed by considering the charge density σ, at the surface of the cavity as defined by the following equation

$$\sigma(P) = -\,\varepsilon_0\frac{\varepsilon - \varepsilon_0}{\varepsilon}\vec{\nabla} V(P)\boldsymbol{n}_-$$

where P is a point on the surface and V is the electrostatic potential at this point, $\boldsymbol{n}_-$ is the inner-unit normal vector of the surface at point P, and ε_0 is the dielectric permittivity of a vacuum.

The shape of the cavity is chosen from the surface on which the electrostatic potential is constant and the enclosed volume is equal to the molecular volume. For compounds (**1**)—(**3**) this quantity has been obtained from a correlation between the experimental molecular volume of the pure liquid at room temperature for a set of structurally related compounds and the Van der Waals volume calculated by the Motoc and Marshall method.[26]

Results and Discussion

Structure and Relative Stability of Isomers.—The relative energies and the main geometrical parameters for the *Z* and *E* isomers of compound (**1**) are shown in Table 1. Geometries have been fully optimized without imposing any symmetry constraints. As can be expected, MNDO strongly underestimates the hydrogen-bonding interaction and gives a very small energy gap between the two isomers. The other semiempirical and *ab initio* calculations agree to within one kcal mol^{-1}. Some features of the geometrical parameters deserve comment. Apart from the long hydrogen-bonding distance given by MNDO for the *Z* isomer, this parameter has two sets of values, one being *ca.* 1.7 Å, from the MNDO/H and STO-3G calculations, and the other being *ca.* 2.0 Å, from the AM1 and 3-21G calculations. This fact implies a different distortion of the groups attached to the double bond. The angles formed by the double bond and the amino and nitro groups, *i.e.* C(2)–C(1)–N(4) and C(1)–C(2)–N(3), in the *Z* configuration are a function of the hydrogen-bonding distance, increasing along with it. The double-bond length calculated by semiempirical methods is larger than that obtained by the *ab initio* calculations. Although the crystal structure of (**1**) has not been determined, the double-bond distance increases on going from *N*,*N*-dimethyl-2-nitroethenamine (1.345 Å)[27] to *N*-methyl-2-nitroetheneamine (1.356 Å),[13] thus suggesting that in the *N*-unsubstituted compound (**1**), the double bond distance should be greater than 1.36 Å, and that the MNDO/H and AM1 predictions are closer to the experimental value.

Table 2 shows the relative MNDO/H and AM1 energy for the four planar isomeric forms of compounds (**2**)—(**7**). According to both methods, the *EE* conformation is strongly disfavoured, and the *ZZ* isomer is predicted to be the most stable conformation, except for compounds (**4**) and (**5**) for which MNDO/H gives nearly the same stability for the *ZZ* and *EZ* isomers. In all cases, the energy of *EZ* isomer remains close

---

* For compounds (**2**)—(**7**) the stereochemistry of each isomer is denoted by two symbols, the first one indicating the configuration around the formal C=C double bond, and the second the orientation around the C(2)–COR^3 bond.

Table 1. Relative energies (kcal mol^{-1}) and main geometrical parameters of *Z* and *E* isomers of 2-nitroethenamine (**1**) (distances in Å and angles in degrees)

	Conformer	MNDO	MNDO/H	AM1	STO-3G	3-21G
E_{rel}	*Z*	0.00	0.00	0.00	0.00	0.00
	E	0.12	4.46	4.00	3.42	4.37
C(1)=C(2)	*Z*	1.369	1.379	1.371	1.338	1.346
	E	1.370	1.370	1.371	1.326	1.335
C(1)-N(4)	*Z*	1.364	1.360	1.348	1.368	1.331
	E	1.372	1.372	1.353	1.383	1.342
C(2)-N(3)	*Z*	1.470	1.467	1.448	1.476	1.401
	E	1.475	1.475	1.453	1.485	1.415
H···O	*Z*	2.456	1.725	2.195	1.694	1.939
C(2)-C(1)-N(3)	*Z*	127.7	120.5	125.4	120.7	122.7
	E	122.4	122.4	121.3	119.0	118.7
C(1)-C(2)-N(4)	*Z*	129.9	122.2	127.7	123.3	128.0
	E	122.2	122.2	124.1	126.0	126.6

Table 2. Relative energy (kcal mol^{-1}) of the planar isomers of compounds (**2**)—(**7**)

Compound	Conformer	MNDO/H	AM1
(**2**)	*ZZ*	0.00	0.00
	ZE	0.59	1.35
	EZ	0.91	0.95
	EE	4.00	4.66
(**3**)	*ZZ*	0.00	0.00
	ZE	1.87	3.28
	EZ	1.12	0.29
	EE	5.24	5.16
(**4**)	*ZZ*	0.02	0.00
	ZE	0.92	6.08
	EZ	0.00	1.63
	EE	15.57	12.48
(**5**)	*ZZ*	0.14	0.00
	ZE	3.84	10.76
	EZ	0.00	0.53
	EE	21.69	12.96
(**6**)	*ZZ*	0.00	0.00
	ZE	0.61	1.36
	EZ	0.94	0.92
	EE	4.29	4.75
(**7**)	*ZZ*	0.00	0.00
	ZE	2.03	3.45
	EZ	1.26	0.25
	EE	5.85	5.52

Table 3. Geometrical parameters of the *ZZ*-isomer of methyl 3-methylamino-2-nitroacrylate (**6**)

Bond lengths/Å	Expt. [ref. (28)]	MNDO/H	AM1
C(1)=C(2)	1.39	1.41	1.39
C(1)-N(4)	1.30	1.35	1.34
C(2)-N(3)	1.41	1.47	1.46
C(2)-C(8)	1.49	1.48	1.47
C(8)-O(11)	1.21	1.23	1.24
C(8)-O(10)	1.32	1.35	1.36
N(3)-O(5)	1.25	1.24	1.21
N(3)-O(6)	1.24	1.20	1.20
O(10)-C(9)	1.44	1.41	1.43
N(4)-C(7)	1.45	1.46	1.43
Standard deviation		0.03	0.03
Bond angles/°			
C(2)-C(1)-N(4)	129	122	128
C(1)-C(2)-N(3)	123	118	124
C(2)-N(3)-O(5)	117	117	119
C(2)-N(3)-O(6)	123	124	120
C(1)-C(2)-C(8)	116	120	116
C(1)-N(4)-C(7)	123	126	122
C(2)-C(8)-O(11)	116	124	125
C(2)-C(8)-O(10)	120	117	117
C(8)-O(10)-C(9)	114	125	116
Standard deviation		6	4

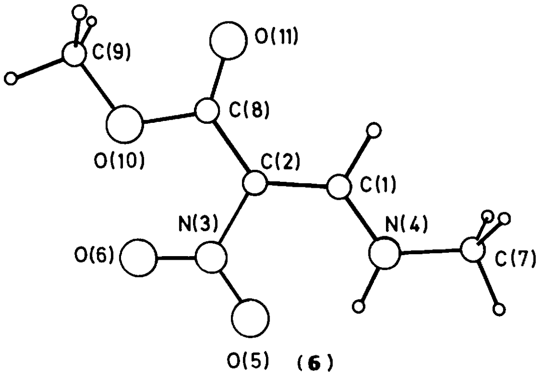

(**6**)

to the *ZZ* isomer energy, whereas the *ZE* energy is close to that of the *ZZ* form for compounds where R^1 = H, but is much higher when R^1 = Me. Comparing (**2**) with (**6**) and (**3**) with (**7**), it can be seen that the relative energies of the isomers remain unchanged by *N*-methyl substitution.

The experimental[28] and the calculated geometrical parameters for the *ZZ* form of (**6**) appear in Table 3. The agreement between the observed and the calculated values is generally satisfactory. Nevertheless, as has been found for compound (**1**), the bond angles of the groups involved in the hydrogen bonding, *i.e.* C(2)–C(1)–N(4) and C(1)–C(2)–N(3), are more distorted in the MNDO/H than in the AM1 geometry, leading to a larger standard deviation of the angle values (6° for MNDO/H and 4° for AM1).

Planar geometries were considered so far in order to give a simplified view of the isomeric equilibria. However, some of the compounds may be more stable by adopting a non-planar arrangement of the ester or acetyl group with respect to the rest of the conjugated system. Calculations of the rotational barrier around the C(2)–COR^3 single bond were performed for the two configurational isomers of compounds (**2**)—(**7**). The curves were calculated for several values of the C(1)–C(2)–CO dihedral angle, keeping planarity constraints for the rest of the conjugated system and optimizing all the remaining parameters. The minima found at intermediate angles were completely optimized. Figure 1 shows the potential curves corresponding to the $ZZ \longrightarrow ZE$ conversion for compounds (**2**) and (**3**)

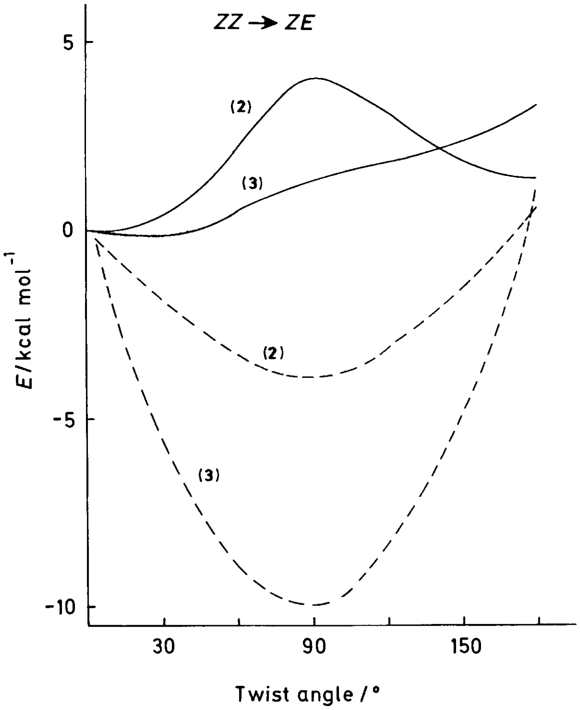

Figure 1. Relative energy upon rotation around the C(2)–COR^3 single bond (AM1 solid line, MNDO/H dashed line)

Table 4. Torsion angle (degrees) of the acetyl or ester group and relative energy (kcal mol^{-1}) of the stationary points of the potential curves to rotation about the C(2)–COR^3 single bond

		Minimum		Maximum	
Compound	Rotation	Angle	E_{rel}	Angle	E_{rel}
(2)	*ZZ* ⟶ *ZE*	0	0.00	90	3.81
		180	1.35		
	EZ ⟶ *EE*	0	0.95	90	6.97
		150	4.50		
(3)	*ZZ* ⟶ *ZE*	30	0.00		
	EZ ⟶ *EE*	0	0.45	90	4.82
		120	3.92		
(4)	*ZZ* ⟶ *ZE*	0	0.00	120	5.87
		150	5.66		
	EZ ⟶ *EE*	0	1.63		
(5)	*ZZ* ⟶ *ZE*	35	0.00		
	EZ ⟶ *EE*	15	0.59		
(6)	*ZZ* ⟶ *ZE*	0	0.00	90	3.78
		180	1.36		
	EZ ⟶ *EE*	0	0.92	90	7.02
		150	4.55		
(7)	*ZZ* ⟶ *ZE*	30	0.00		
	EZ ⟶ *EE*	0	0.59	90	4.58
		150	4.24		

computed by the MNDO/H and AM1 methods. As can be seen MNDO/H favours a perpendicular or nearly perpendicular orientation of the ester group, contrary to the AM1 predictions. Previous MNDO calculations[16,23,29] on similar molecules have shown that this method typically favours structures in which the two conjugated parts of the system are mutually perpendicular or nearly perpendicular; on the other hand, experimental evidence[19,28] indicates that AM1 structural predictions are more realistic. Table 4 presents data concerning the angle and relative AM1 energy of the stationary points obtained for each interconversion barrier. The zero-energy level corresponds to the most stable structure for each compound. The zero value of the torsional angle corresponds to the planar structure of the first isomer indicated in the *rotation* column, *e.g.* *ZZ*(0°) ⟶ *ZE*(180°). The results indicate that some planar conformations are not really minima. Actually, when a methyl group is attached to C(1) [compounds **(3)**, **(5)**, and **(7)**], the energy minima do not correspond to the *ZZ* and *ZE* conformations, but to an intermediate disposition where the ester or acetyl group is twisted out of the plane. This important structural change is not followed by a strong energy change in the new minima, due to the near planarity of the potential surface in this region. In contrast, the *EZ* isomer remains as the minimum for all the compounds, except for the 4-amino-3-nitropent-3-en-2-one **(5)**, where a 15° twist angle is found.

The experimental results were obtained in solution, whereas this fact was not considered in the above calculations. Owing to the small energy gap between the different isomers, solvent effects may change the relative populations of isomers, especially if the large difference between the charge spatial distribution of the different isomers is taken into account. Solvation energies of compounds **(1)**—**(3)** have been calculated at the MNDO/H level by the continuum model described above. Table 5 shows the molecular volume, dipole moment, solvation energy, and new relative energies of each isomer. Dielectric permittivities of chloroform (4.8), methanol (32.7), and dimethyl sulphoxide (46.7) were used. It is remarkable that the major change in the relative energy is obtained when passing from the gas phase to solution, although the dielectric permittivity values are quite different. For compound **(1)** the energy gap between both isomers is highly diminished, leading to an increase in *E*-isomer population as the polarity solvent is increased. For compound **(2)** the *ZE* isomer is more highly favoured by the solvation and thus becomes the most stable. For compound **(3)** the new relative energies lead to a population ratio where *ZZ*: *EZ* is *ca.* 1.

Inspection of Table 5 shows that the solvation energy of some isomers does not correlate well with their dipole moments, and the explanation for this probably lies in the contribution of the multipole moments. The importance of this contribution will increase as the number of substituents on the nitro enamine increases. Thus, for **(1)** the correlation is fairly good, while for **(2)** it is only partial, and it does not exist for tetrasubstituted ethylene **(3)**.

At this point, it is worth commenting on the ability of the methods used to predict the structural and energetic aspects of the isomeric equilibria. First of all, the calculated geometries quite agree with the experiment. On one hand, the quantitative comparison for **(6)** (Table 3) leads to typical deviation slightly above experimental error while on the other, qualitative information on stable structures agrees quite well with the results shown in Table 4. Compounds **(3)**, **(5)**, and **(7)** with a methyl group attached at C(1) only have a configurational *Z* isomer which is an intermediate structure between the *ZZ* and *ZE* conformations. As seen in Figure 1, MNDO/H fails to predict the proper orientation of the ester and acetyl group when they are not hydrogen bonded. This limitation is removed by AM1, thus suggesting that this new parametrization introduces modifications with respect to MNDO beyond that of the hydrogen bond.

At first sight, the calculated population ratio seems to be less satisfactory than the geometric predictions. Nevertheless, it must be pointed out that the energy gap between the stable isomers is, in most cases, to within one or two kcal mol^{-1} and the intrinsic errors of these semiempirical methods are near to this value. Moreover, solvation energy must be taken into account in order to offer a more realistic representation of the equilibria, as this correction is along the same order as the energy gap. Thus considering compound **(1)**, the inclusion of a corrective term for accommodating hydrogen-bonding interactions in

Table 5. Solvation energy and new relative energy in solution (in kcal mol^{-1})

				E_{solv}			E_{rel}^{total}			
Compound	Isomer	Molecular volume/Å^3	Dipole moment/D	ε = 4.8	ε = 32.7	ε = 46.7	ε = 1.0	ε = 4.8	ε = 32.7	ε = 46.7
(1)	*Z*	135.5	5.91	−8.18	−11.04	−11.21	0.00	0.00	0.00	0.00
	E		7.09	−10.71	−14.34	−14.55	4.46	1.93	1.16	1.12
(2)	*ZZ*	223.2	4.42	−12.44	−17.02	−17.28	0.00	0.29	0.59	0.61
	ZE		7.37	−13.32	−18.20	−18.48	0.59	0.00	0.00	0.00
	EZ		5.79	−12.26	−16.73	−16.99	0.91	1.38	1.79	1.81
	EE		8.74	−12.57	−17.05	−17.31	4.00	3.87	4.56	4.58
(3)	*ZZ*	251.3	4.72	−9.79	−13.44	−13.66	0.00	0.00	0.03	0.03
	ZE		7.54	−10.17	−13.91	−14.12	1.87	1.49	1.43	1.38
	EZ		5.80	−10.65	−14.59	−14.81	1.12	0.26	0.00	0.00
	EE		8.77	−11.44	−15.59	−15.83	5.24	3.59	3.12	3.10

Table 6. Energy barrier (kcal mol^{-1}) to rotation about the double bond for the *ZZ* ⟶ *EZ* isomerization

Compound	Method	$\Delta E^{\ddagger}$
(1)	MNDO/H	36.8
	AM1	37.2
(2)	MNDO	17.4
	MNDO/H	26.4
	AM1	27.8
(3)	MNDO	7.9
	MNDO/H	20.5
	AM1	20.6
(4)	AM1	26.3
(5)	AM1	17.6
(6)	AM1	26.8
(7)	AM1	18.7

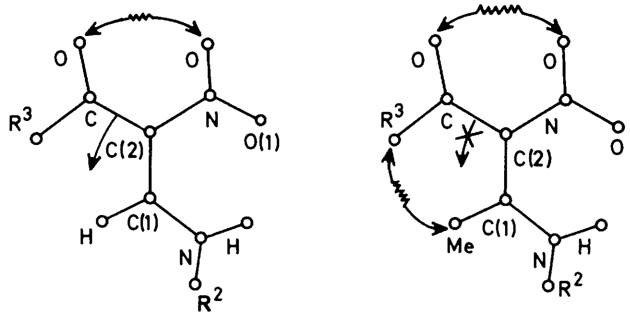

Figure 2.

MNDO raises the energy gap between the two configurations to 4 kcal mol^{-1} (Table 1). From this result the conclusion is that hydrogen-bonding interaction is the main factor in determining the population ratio and it would be expected that the *Z*-isomer is the sole configuration to be detected. Nevertheless, the addition of solute–solvent electrostatic interactions leads to a decrease in the energy gap of *ca.* 3 kcal mol^{-1}. Thus the *Z*:*E* ratio is predicted to be 5:1 in a dielectric continuum of the same polarity as that of dimethyl sulphoxide. This result still overestimates the *Z* population, though it must be noted that specific solute–solvent interactions have not been considered in these calculations. It is expected that in solvents able to form hydrogen bonds, such as dimethyl sulphoxide and methanol, the energy gap will decrease, given that the solute–solvent hydrogen bonds will weaken the intramolecular bond of the *Z* isomer.

For the remaining compounds, the energy gap suggests an equilibrium between the *EZ* isomer and a configurational *Z* isomer, which may be the wholly planar *ZZ*-form or a twisted one with the ester or acetyl group *ca.* 30° out of the plane of the nitro enamine system. The *ZE* conformation is involved in the equilibrium only when R^1 = H, that is, when the repulsion between the oxygen lone pairs of the nitro and carbonyl group can be relieved by the in-plane bond deformation shown in Figure 2. For **(4)** and **(5)**, the greater charge density on the acetyl oxygen relative to that existing in the ester carbonyl oxygen brings about a further destabilization of the *ZE* isomer.

As shown for **(1)**, when solvent effects are included in the calculations for compounds **(2)** and **(3)**, the results of isomer ratio are modified as suggested by the experiment.

Rotational Barriers around the Double Bond.—Table 6 shows the rotational barrier around the double bond for the *ZZ* ⟶ *EZ* interconversion. For all the compounds, the maximum is found for a torsional angle of 90° and, as anticipated for push–pull ethylenes, the barriers are lower than those of simple ethylenes (62—65 kcal mol^{-1}).[30] Furthermore, the energy barrier is diminished by a second electron-withdrawing group on C(2), and this effect is stronger for the acetyl than for the ester group. The data in Table 6 also show that the energy barrier is lowered by the methyl substitution on C(1) (by *ca.* 8 kcal mol^{-1}), and to a lesser extent by *N*-methyl substitution (by *ca.* 1 kcal mol^{-1}). The results for compounds **(2)** and **(3)** show the similarity between the MNDO/H and AM1 predictions, and the lower values provided by MNDO. Figure 3 shows the shape of the rotational barriers obtained by the three semiempirical methods for compound **(3)**. As previously mentioned, the MNDO results may be explained by the poor estimation of hydrogen bonding given by this method. In fact, the small barrier values are a consequence of the minor stabilization of the curve minima, where intramolecular hydrogen bonding exists, but are poorly described. Moreover, the predicted MNDO minima for **(3)** are found at 30 and 150° twist angles.

Comparison of MNDO/H and AM1 barriers with experiment indicates that the theoretical results are overestimated by *ca.* 7—10 kcal mol^{-1}. Nevertheless, the predicted general behaviour is followed qualitatively. The increase in the energy barrier with the substituent on C(2) in the order COMe < CO_2Me < H is accounted for. The C(1) methyl substitution greatly diminishes the barrier height, whereas the *N*-methyl substitution causes only a slight decrease in the barrier value. A strong correlation is found between the barrier values and the C(1)–C(2) bond order of the initial state, *i.e.* the *ZZ* isomer. According to the double-bond order, the compounds may be grouped in three sets. The first one includes only compound **(1)**, which has the greatest bond order (1.60) and the highest barrier. The second set contains the compounds with R^1 = H, which have intermediate barrier values and bond orders, *i.e.* **(2)** (1.45), **(4)** (1.44),

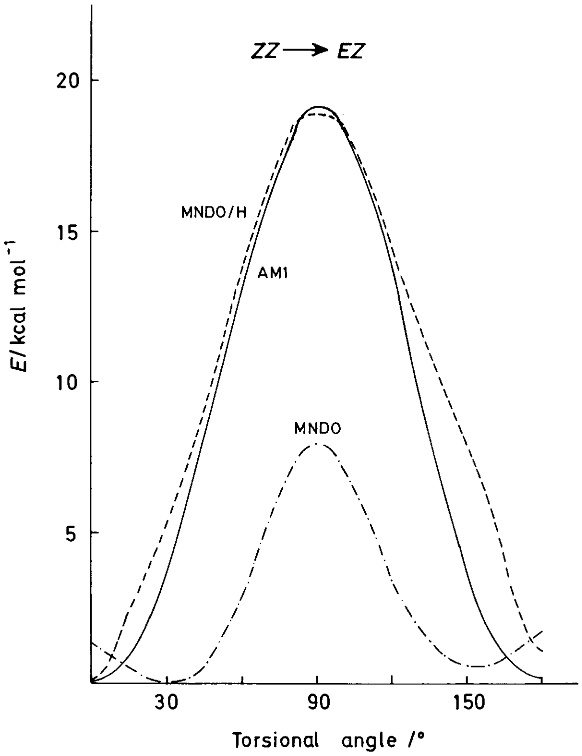

Figure 3. Relative energy upon rotation around the C=C double bond for compound (**3**)

and (**6**) (1.44). The third group includes the compounds with R^1 = Me, which have the lowest barriers and the smallest bond orders, *i.e.* (**3**) (1.40), (**5**) (1.41), and (**7**) (1.39). This correlation seems to indicate that the main factor discriminating between the barrier heights is the order of the C–C bond in the initial state. This fact is not surprising since the two groups which have a more important role in stabilizing the transition state, *i.e.* NO_2 and NHR, are present in all the compounds studied.

The rotational barrier heights depend on the nature of the solvent.[5–7,10] Owing to the large charge separation in the transition state, an increase in the dielectric constant of the medium reduces the energy barrier. Calculations at the CNDO/2 level of the solvent effect on the rotational barriers of some 6,6-disubstituted fulvenes[31] have been performed by means of the reaction-field formalism considering the dipole moment of the initial and transition state. The values obtained (5—10 kcal mol^{-1}) depended on the cavity radius. These results point out that the correction of the electrostatic solute–solvent interactions is of the same order of magnitude as the gap between our theoretical results and the experimental values. Preliminary calculations[32] of the barriers for (**2**) and (**3**), taking into account the solvation, give a better agreement with experiment.

In conclusion, the MNDO/H and AM1 semiempirical calculations supply a reasonable description of the isomeric equilibrium of the nitro enamines studied. Geometrical parameters agree with experiment, with AM1 being more adequate than MNDO/H for describing the disposition of the ester and acetyl group. The isomer population ratio is qualitatively predicted, whereas the energy barriers around the double bond are systematically overestimated, the main cause of the discrepancy probably being the solvation contribution rather than the inaccuracy of the semiempirical methods. The inclusion of electrostatic solute–solvent interactions improves the results. A better and more complex picture should also take in consideration the acid–base properties of the solvent which can change the *Z,E* isomerization mechanism, particularly when the enamine has an N–H bond. Future efforts should be focussed not only on obtaining more accurate wavefunctions but also on introducing a more complete description of the solvent effect by including specific solute–solvent interactions.

Acknowledgements

This work is a part of a research project supported by the Comisión Asesora de Investigación Científica y Técnica and the Consejo Superior de Investigaciones Científicas of Spain, to which we express our gratitude.

References

1 S. Rajappa, *Tetrahedron*, 1981, **37**, 1453.
2 A. Krowczynski and L. Kozerski, *Heterocycles*, in the press.
3 K. Fuji, M. Node, H. Nagasawa, Y. Naniwa, and S. Terada, *J. Am. Chem. Soc.*, 1986, **108**, 3855.
4 A. Gómez-Sánchez, F. J. Hidalgo-Garciá, J. L. Chiara, and J. Bellanato, *An. Quim.*, 1985, **81C**, 139; A. Gómez-Sánchez, F. J. Hidalgo-Garcia, and J. L. Chiara, *Carbohydr. Res.*, 1987, **167**, 55; *J. Heterocyclic Chem.*, 1987, **24**, 1757
5 J. Sanström, *Top. Stereochem.*, 1983, **14**, 83.
6 U. Berg and U. Sjostrand, *Org. Magn. Reson.*, 1978, **11**, 555.
7 K. I. Dahlquist, *Acta Chem. Scand.*, 1970, **24**, 1941.
8 I. Belsky, H. Dodiuk, and Y. Shvo, *J. Org. Chem.*, 1977, **42**, 2734.
9 H. O. Kalinowski, H. Kessler, and A. Walter, *Tetrahedron*, 1974, **30**, 1137.
10 V. I. Bakhmutov and E. I. Fedin, *Bull. Magn. Reson.*, 1984, **6**, 142.
11 V. I. Bakhmutov and V. A. Burmistrov, *Org. Magn. Reson.*, 1979, **12**, 185.
12 V. I. Bakhmutov, K. K. Babievsky, V. A. Burmistov, E. I. Fedin, and V. M. Belikov, *Izv. Akad. Nauk SSSR*, *Ser. Khim.*, 1978, 2719.
13 E. N. Gate, M. A. Meek, C. H. Schwalbe, M. F. G. Stevens, and M. D. Threadgill, *J. Chem. Soc., Perkin Trans. 2*, 1985, 251.
14 Yu. A. Borisov, K. K. Babievskii, V. I. Bakhmutov, Yu. T. Struchko, and E. I. Fedin, *Izv. Akad. Nauk SSSR*, *Ser. Khim.*, 1982, 123.
15 J. Sandström, in 'Dynamic NMR Spectroscopy,' Academic Press, London, 1982, ch. 10.
16 G. Favini, A. Gamba, and R. Todeschini, *J. Chem. Soc., Perkin Trans. 2*, 1985, 915.
17 A. Krowczynski and L. Kozerski, *Synthesis*, 1983, 489.
18 J. L. Chiara, Tesis de Licenciatura, Sevilla, 1985; J. L. Chiara and A. Gómez-Sánchez, unpublished results.
19 J. L. Chiara, A. Gómez-Sánchez, F. J. Hidalgo, and J. Bellanato, *J. Chem. Soc., Perkin Trans. 2*, 1988, 1691.
20 T. Tokumitsu and T. Hayashi, *Nippon Kagaku Kaishi*, 1983, 88.
21 M. J. S. Dewar and W. Thiel, *J. Am. Chem. Soc.*, 1977, **99**, 4899, 4907.
22 K. Y. Burshtein and A. N. Isaev, *Theor. Chim. Acta*, 1984, **64**, 397.
23 M. J. S. Dewar, E. G. Zoebisch, E. F. Healy, and J. J. P. Stewart, *J. Am. Chem. Soc.*, 1985, **107**, 3902.
24 J. L. Rivail, B. Terryn, D. Rinaldi, and M. F. Ruiz-Lopez, *J. Mol. Struct.* (*THEOCHEM.*), 1985, **120**, 387.
25 S. Miertus, E. Scrocco, and J. Tomasi, *Chem. Phys.*, 1981, **55**, 117; S. Miertus and J. Tomasi, *Chem. Phys.*, 1982, **65**, 239; R. Bonacorsi, C. Ghio, and J. Tomasi, *Stud. Phys. Theor. Chem.*, 1982, **21**, 407.
26 I. Motoc and G. Marshall, *Chem. Phys. Lett.*, 1985, **116**, 415.
27 A. Hazell and A. Mukhopadhyay, *Acta Crystallogr., Sect. B*, 1980, **36**, 747.
28 V. G. Andrianov, Yu. T. Struchkov, and K. K. Babievsky, *Cryst. Struct. Commun.*, 1982, **11**, 35.
29 P. Birner and H. J. Hoffmann, *Int. J. Quantum Chem.*, 1982, **XXI**, 833.
30 J. E. Douglas, B. S. Rabinovitch, and F. S. Looney, *J. Chem. Phys.*, 1955, **23**, 315; B. S. Rabinovitch and K. W. Michel, *J. Am. Chem. Soc.*, 1959, **81**, 5056; R. B. Cundall and T. F. Palmer, *Trans. Faraday Soc.*, 1961, **57**, 1936; K. J. Laidler and M. C. Lin, *Can. J. Chem.*, 1968, **46**, 937.
31 T. Olsson and J. Sandström, *Acta Chem. Scand., Ser. B*, 1982, **36**, 23.
32 R. R. Pappalardo and E. Sánchez Marcos, to be published.

Received 15*th January* 1988; *Paper* 8/00196